Multi-Modal Graph-Based Machine Learning for Predicting Surgical Outcome in Epilepsy Patients

Artur Arturi Aharonyan[1,2*], Syeda Abeera Amir[1*], Nunthasiri Wittayanakorn[3], Marius George Linguraru[1,4], Chima Oluigbo[3], Syed Muhammad Anwar[1,4**]

[1]Sheikh Zayed Institute for Pediatric Surgical Innovation, Children's National Hospital, Washington DC, USA
[2]The Catholic University of America, Washington DC, USA
[3]Department of Neurological Surgery, Children's National Hospital, Washington DC, USA
[4]George Washington University, Washington DC, USA
**sanwar@childrensnational.org

Abstract. Reliable prediction of seizure outcomes after surgical intervention before ablative surgery could play a critical role for tailoring epilepsy treatment. However, for diverse patient populations, accurate and personalized predictions remain challenging with traditional methods. Current methods rely heavily on clinical expertise and experience, and data driven tools may help in supporting clinicians to make more informed surgical decisions. This study presents a novel deep learning-based spatio-temporal graph neural network (ST-GNN) model to predict reduction in seizure frequency utilizing high-quality stereo electroencephalography (sEEG) and structural magnetic resonance imaging (MRI) data. sEEG and MRI data are curated from patients with pharma-coresistant refractory epilepsy and suspected wide/complex seizure networks or multifocal epilepsy. A total of 10 pediatric patients with sEEG contacts in the thalamus were considered, where data from multiple ictal events was used to train the model. Our ST-GNN model integrates local and global connectivity using graph convolutions with multi-scale attention mechanisms to capture patterns between difficult-to-study regions such as the thalamus and cortical/subcortical regions, both from MRI and sEEG. The model achieved an accuracy of 90.4%, and 75.4% in predicting seizure outcomes for seizure-wise and patient-wise prediction respectively. Edge-level connectivity analysis highlighted the thalamus and mid insula regions as key regions. Our findings underscore the potential of new connectivity-based deep learning models leveraging multimodal data for enhancing the prediction of seizure outcomes and tailoring treatment planning for epilepsy. Our multi-modal approach can help inform AI-assisted personalized epilepsy treatment planning. Code is available on our GitHub.

Keywords: sEEG, deep learning, seizure frequency, epilepsy, graph learning.

[*] Denotes equal contribution

1 Introduction

Epilepsy affects approximately 50 million people worldwide, with nearly one-third experiencing drug-resistant epilepsy (DRE), where seizures persist despite multiple anti-seizure medications [1]. There is strong evidence that surgery can be highly effective in reducing seizure frequency and improving quality of life in patients with DRE [2]. However, effectiveness of ablative surgery remains difficult to predict and is highly dependent on the experience of the clinical team and various observations including imaging, physiological data and neurophysiological evaluations guiding the decisions.

Success of epilepsy surgery heavily depends on the accurate identification of the seizure onset zone (SOZ) and its epileptogenic network. The prediction of seizure outcomes after surgery has remained challenging especially for those with suspected wide/complex seizure networks or multifocal epilepsy where resection or ablation is not an option [3]. This critical need for accurate outcome prediction has driven research into developing sophisticated analytical approaches [4]. Intracranial observations using stereo-electroencephalography (sEEG) and subdural grids implantation, and non-invasive magnetic resonance imaging (MRI) are widely used methods for identifying the lesions and underlying seizure networks causing ictal events. For cases where such lesions are not seen on MRI scans, sEEG is used for more conclusive observations and identification of the epileptogenic zone [5]. MRI provides detailed anatomical images of the brain, aiding not only in identifying structural abnormalities but also guiding sEEG trajectory planning. sEEG offers deep brain recording capabilities with high temporal resolution and is often used to identify discrete neocortical SOZs. Among the subcortical regions involved in the propagation of seizures, thalamic nuclei have repeatedly shown interconnectedness with ictal brain regions [6–8]. In a study investigating energy distribution between temporal cortices and the anterior nucleus of thalamus (ANT) across seizure stages, the average thalamic power was found to be significantly higher at seizure onset compared to baseline power [9].

Sampling of thalamic targets during sEEG is a developing area of surgical epilepsy clinical practice. The increasing inclusion of thalamic recordings has opened new avenues for understanding thalamocortical networks, which are fundamental to both developing brain function and pathological states [7]. Moreover, traditional visual analysis of sEEG recording often struggles to capture the thalamic signatures involved in the complex, interconnected nature of epileptic networks, particularly the subtle thalamic seizure onset patterns [8, 10]. Graph Neural Networks (GNNs) present a promising approach for analyzing such complex neural data, as they can model the brain's networked structure and capture both local and global connectivity patterns [11, 12]. In graph-based applications, brain regions are represented as nodes, and the strength of their connections as edges, hence enabling the representation of connectivity patterns. Therefore, unlike traditional machine learning approaches, GNNs can explicitly incorporate spatial relationships and non-linear interactions between brain regions, making them particularly well-suited for analyzing thalamocortical connectivity patterns in epilepsy.

In this paper, we present a novel multi-modal spatio-temporal GNN-based classifier model for predicting seizure outcomes using sEEG, with thalamic sampling and MRI data from patients with suspected wide epileptic networks or multifocal epilepsy. Our

method combines temporal precision and structural mapping, offered by sEEG and MRI, respectively, to develop a GNN that can capture the complex interactions between various brain regions, especially the critical connections between the thalamus and cortical structures. We also applied our model to study connectivity during seizures and identify the most important brain regions for the seizure outcome classification task. Our approach provides valuable insights into poorly understood seizure dynamics, such as the relationship between seizure onset zones and seizure networks.

2 Methodology

The proposed methodology is shown in Figure 1, where we incorporate multimodal graph learning to predict seizure outcomes in pediatric patients.

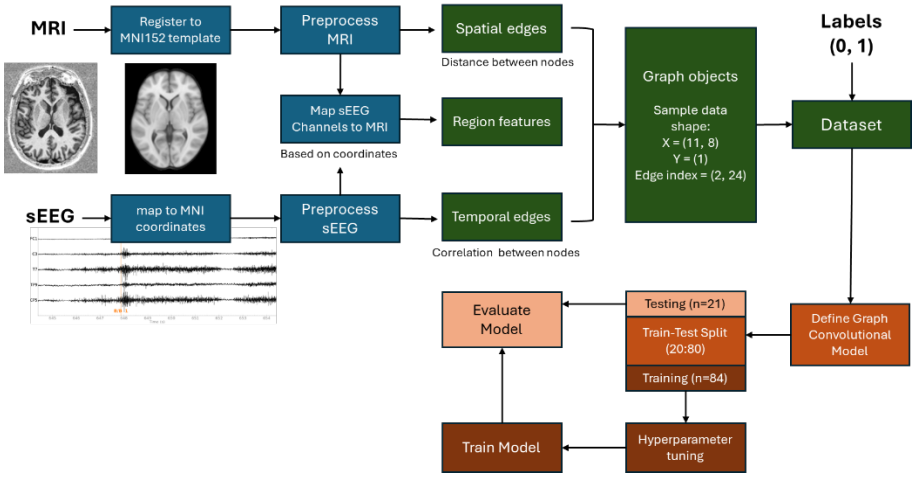

Figure 1: Overview of the proposed pipeline integrating sEEG and MRI data to predict seizure outcomes in pediatric epilepsy. X and Y in Graph objects refer to the node feature matrix, where X refers to nodes and features and Y is the graph label. The edge index matrix is the connectivity of the graph.

2.1 Patient Selection

This is a retrospective study performed on 10 consecutive pediatric patients with pharmacoresistant epilepsy who underwent sEEG with thalamic interrogation and subsequently underwent the definitive procedures for epilepsy at our medical center from July 2023 to August 2024. The seizure outcomes were recorded at 6 months follow up post-surgery. The study was conducted under the Institutional Research Board's (IRB) approval without written consent required from all included patients. All data were obtained in routine clinical care. Relevant clinical information such as demographics, semiology, etiology, preoperative testing, results in noninvasive epilepsy investigations, details of sEEG procedure, definitive epilepsy surgery after sEEG, and seizure outcome

at the last follow-up were extracted from patient records. The clinical outcomes and sEEG data were analyzed to identify patterns indicating thalamic nuclei involvement in observed epilepsy networks.

The sEEG electrodes targeting thalamic nuclei, including the anterior nucleus of thalamus (ANT), centro-median nucleus (CM), or pulvinar (PUL), were selected based on the suspected SOZs and the known anatomical connectivity of thalamic nuclei. Post-operative computed tomography scans were used to segment and reconstruct each depth electrode targeting a thalamic nucleus. ROSA ONE Brain and Surgical Theater was utilized for accuracy, particularly in identifying the number of contacts successfully placed within each nucleus. Any electrode contacts located outside the planned thalamic subdivision were excluded from the analysis.

MRI data was collected with an 8-channel head coil on a 3T General Electric scanner. A gradient echo pulse sequence was used with 3mm isotropic voxels, repetition time = 2s, flip angle = 90deg, and in-plane field of view = 192 x 192 mm. Data was collected as part of an ongoing clinical research dataset and was approved by the IRB at Children's National Hospital. The reported outcome from self or caregiver at the last follow-up was noted in patients at least six months after the definitive procedure for epilepsy. These outcomes were classified as: (1) seizure-free, complete elimination of seizures; (2) excellent, >80% reduction in seizure frequency; (3) good, >50% reduction in seizure frequency; (4) poor, <50% reduction in seizure frequency; and (5) worse, worsening of seizures and/or unacceptable neurologic deficit [13]. The study categorized patients into two groups based on percentages of seizure frequency reduction described. Group I (class 1), which includes patients with more than 50% seizure reduction, consisted of 3 patients. Group II (class 0), with patients experiencing less than 50% seizure reduction, included 7 patients. In total, the study included 10 patients and 105 ictal events.

2.2 Data Pre-processing

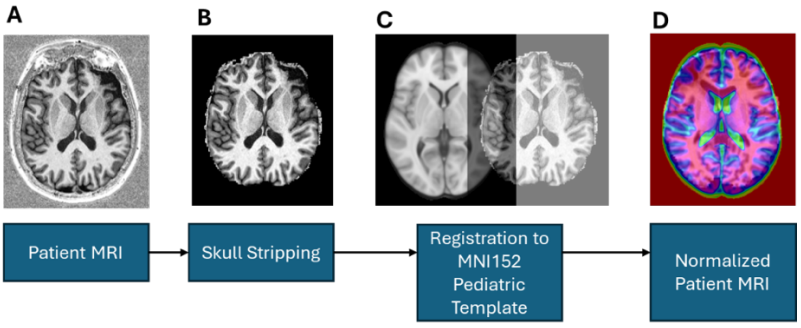

Figure 2: The pre-processing for neuroimages pipeline. (A) Original patient MRI, (B) skull-stripped image, (C) registration of patient to template, (D) final normalized image.

The overall per-processing pipeline is shown in Fig. 2. For all patients, neuroimaging MRI data were skull-stripped with 3D Slicer and registered non-linearly with rigid transformation to the Montreal Neurological Institute (MNI) 152 T1-weighted brain template with MIPAV [14–17]. MNI is commonly used in neuroimaging to align and compare brain images from different individuals. The purpose of normalization involves transforming individual MRI scans to this common reference space, ensuring that anatomical features are consistently aligned across different subjects. This process facilitates reliable comparison and analysis in neuroimaging studies by removing variability and enhancing the reproducibility of findings across different studies and research groups by aligning regions of interest (ROIs). The resulting structural MRIs of each patient were in normalized space and served as the foundation for the initial graph structure. sEEG pre-processing was conducted with MNE-Python [18]. The raw signal underwent several pre-processing steps: resampling to 128 Hz, normalization by subtracting the mean and dividing by the standard deviation and padding each sample to 5,000 time points. After preprocessing, data was aligned with its corresponding MRI-derived ROIs by anatomical region-based coordinates in MNI space that were manually annotated. The channels were then grouped into ROIs and used as nodes in graph construction.

2.3 Model Development and Testing

Following preprocessing, sEEG and MRI data were structured into graph representations, where each brain ROI served as a node. Temporal edges were established between nodes based on sEEG correlation patterns, while spatial edges were based on distance between nodes, integrating both structural and functional connectivity. The model architecture consisted of two graph layers using graph attention networks (GAT), with each layer using 4 attention heads to capture different aspects of node relationships. Feature analysis leveraged the attention mechanisms intrinsic to the GAT architecture to identify important brain regions. The attention coefficients revealed which nodes were most influential in the model's decision process by measuring how strongly each region attended to others in the graph. The data was then analyzed for correlation between channels by Pearson Correlation given as $p = Cov\ (\frac{X,Y}{\sigma_X \sigma_Y})$, where X and Y are the channel pairs analyzed for correlation. The correlations were visualized in a graph network to compute thalamic nodes' eigenvector centrality using $x_v = \frac{1}{\lambda}\sum_{t \in G} a_{v,t} x_t$, where $a_{v,t}$ is the adjacency matrix, x_t is the eigen vector of a, λ is the largest eigen vector, and G is the set of vector neighbors; and network density $\rho = \frac{2E}{n(n-1)}$, where E is the number of connections (edges) in the network and n is the total number of nodes.

3 Experiments and Results

We conducted multiple experiments to compare our model's performance in detecting seizure outcomes. The model performance is evaluated using metrics including

accuracy, precision, recall and F1 score. We conducted experiments to evaluate the effectiveness of leveraging multimodal data. We also evaluated the model performance using data from 1) ictal events and 2) patient-wise approach. Both experiments were compared against our multimodal pipeline as shown in Fig 1. For the patient-wise analysis, we employed a Leave-One-Out cross validation (LOOCV) approach, sequentially training the GNN model on all patient graphs except for one patient, which was used as the test case. Hyperparameter tuning with 20 trials and 50 epochs per trial was done using Optuna. Class weight computation was done using sklearn to account for class imbalance in the data. ReLU activation functions and dropout (rate 0.21) were applied after each layer, followed by global mean pooling for node feature aggregation.

Training was optimized using the cross-entropy loss function and the Adam optimizer. The model was trained for 100 epochs. To rigorously assess the model's performance, 10-fold stratified cross-validation was employed. The dataset was systematically divided into 10 equally sized subsets, with each subset serving as a held-out test set in turn. Performance metrics were calculated for each fold and subsequently averaged for accuracy, precision, recall and F1-score. Training was conducted on a Nvidia RTX A5000 GPU, with a total runtime of approximately one hour.

Table 1. Results from our pipeline predicting reduction in seizure frequency.

	Multimodal	**sEEG Only**	**Patient-Wise**
Accuracy	90.4%	77.1%	75.4%
Precision	93.1%	69.2%	80.0%
Recall	90.4%	77.1%	75.4%
F1	90.9%	71.7%	77.5%

Table 1 shows a summary of the performance metrics and shows our multimodal strategy demonstrated strong classification performance across multiple evaluation metrics. It achieved an accuracy of 75.4% for patient-wise analysis. In seizure-wise classification using multimodal data the accuracy is 90.4%, while without MRI, accuracy was 77.1%. The lower performance in patient-wise analysis is attributed the smaller number of patients included in the study. We also clearly see that the performance improves when multimodal data is used to make outcome prediction. This lays the groundwork to include functional MRI data in future studies for further improvements in prediction performance.

4 Discussion

Figure 3 shows the regions identified as most important during classification, with the highest values being of the mid insula and thalamus. Figure 4 shows the sEEG connectivity in the thalamocortical network engaged during seizure onset and at seizure end, for patients with high (class 1) or low reduction (class 0) in seizure frequency. The network graphs show a stronger correlation between cortical and thalamic channels in patient with lower reductions during seizure onset, with network density of 1 compared

to 0.4 in patient with greater reduction. Class 0 had greater network differences between start and end of seizure (density = -0.03, average centrality = -0.6) than class 1 (density = -0.01, average centrality = -0.2). The average eigenvector centrality of thalamic nodes was similar (A = 0.44, B = 0.4) for both at seizure onset and seizure end (A = 0.32, B = 0.3).

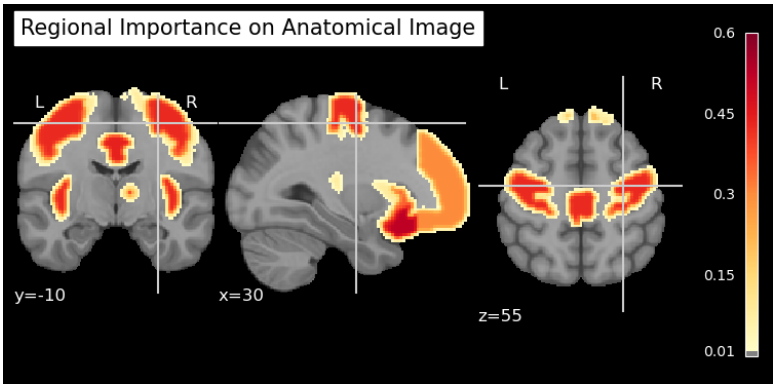

Fig. 3. Node importance map for seizure outcome classification identified through attention in our model. The feature analysis reveals that the model attends the most to the thalamus (MFCM = 0.113) and mid insula (SCMI = 0.131), with the rest 9 regions falling in the range 0.037-0.057.

Our study cohort is unique, and it is rare to find high quality signals from such deep parts of the brain such as thalamus. Compared to typical recordings, this high-quality sEEG data with thalamic implantation provides a much more detailed and precise representation of the brain's electrical activity and connectivity with the cortical regions. This level of detail is crucial for accurately identifying the complex neural networks involved in seizure activity and for making informed decisions about surgical interventions. Predicting the outcome pre-surgery can help clinicians decide on the most effective course of treatment to achieve higher reduction in seizure frequency for difficult patients. This predictive capability is especially valuable in tailoring surgical approaches to individual patients. While we show the potential of utilizing multimodal data for brain connectivity analysis (accuracy increasing by 13.3%, when compared to sEEG only) in pediatric epilepsy with complex seizure networks, our study has several limitations.

During registration, the deformations in some of the patient brains presented challenges arising from the variability in pediatric brain related to age and limited availability of appropriate atlases. For example, in the final registered image in Figure 2, the ventricles don’t fully align with the template due to the gross deformation on the right side. Hence, there is a need for improved registration techniques to ensure precise three-dimensional analysis. Further, variations in individual patient characteristics, such as the type of epilepsy, may not be fully captured in a small sample size such as ours. It is important to acknowledge that our current model, while promising, will need further refinement to account for these individual differences, though our model demonstrates the validity of using MRI with sEEG to predict surgical outcomes.

Future studies that include larger and non-pediatric patient populations can refine the

model's performance, increasing its applicability and reliability in different clinical settings. Expanding the sample size would also enable the exploration of more nuanced patterns and relationships within the data, ultimately enhancing the model's predictive capabilities and clinical utility as a component of an AI-assisted pipeline for seizure network analysis and surgical guidance.

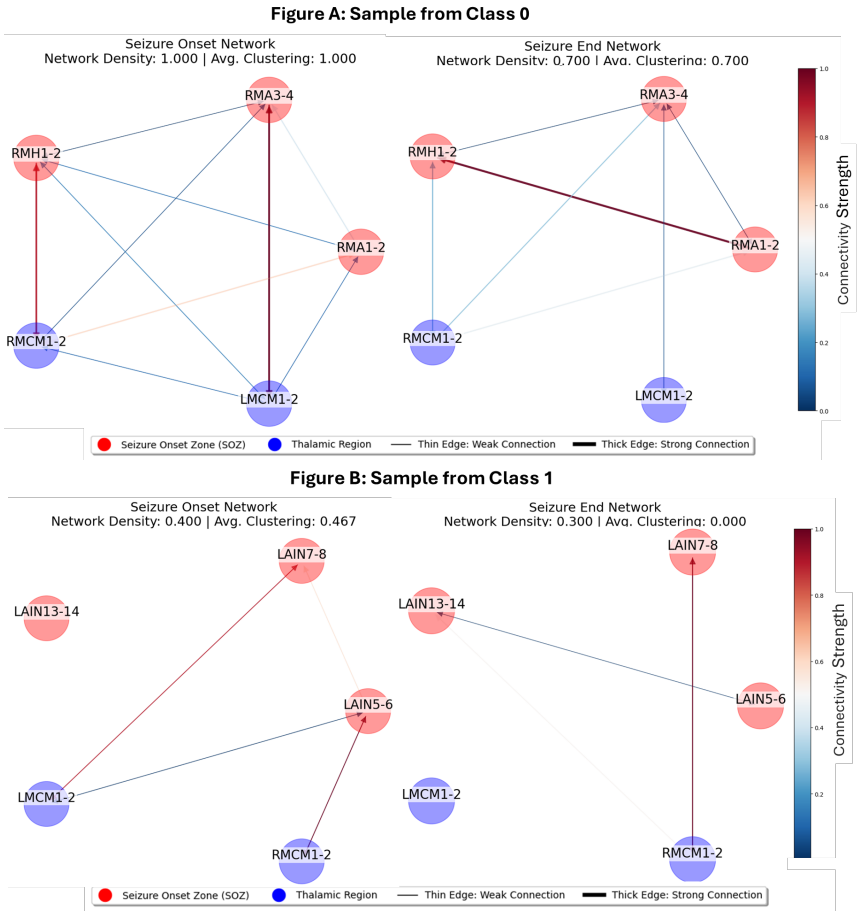

Fig. 4. Comparison of network connectivity between a sample patient from class 0 (A) and class 1 (B) at seizure onset and seizure end. The blue nodes represent the thalamus (RMCM, LMCM) with the following cortical regions: Anterior Insula (LAIN); Amygdala (RMA); Hippocampus (RMH).

5 Conclusion

Our study presents a pioneering pipeline for predicting epilepsy surgery outcomes and understanding seizure dynamics in patients with refractory epilepsy and complex

seizure networks using a multi-modal approach. Our results demonstrate high accuracy for binary-class prediction of seizure outcomes in terms of seizure frequency reduction, as well as patient-wise analysis. Our model is developed for patients with complex seizure networks with demonstrated involvement of thalamus region using sEEG data. The channels identified as important by the model matched those channels clinically identified as the SOZs, adding credence to our results. The implications of this work extend beyond predicting a reduction in seizure frequency; GNNs such as the one we developed may help guide future research to understand the connectivity of the brain and how the brain reacts to disruptions in its connectivity networks during traumatic neurological events such as seizures, traumatic brain injury, and diffuse axonal injury.

Disclosure of Interests. There are no conflicts of interest.

Acknowledgment: This study is funded in part by the Chief Academic Officer (CAO) pilot grant from Childrens National Hospital, Washington DC.

References

1. Fiest, K.M., Sauro, K.M., Wiebe, S., Patten, S.B., Kwon, C.-S., Dykeman, J., Pringsheim, T., Lorenzetti, D.L., Jetté, N.: Prevalence and incidence of epilepsy: A systematic review and meta-analysis of international studies. Neurology. 88, 296–303 (2017). https://doi.org/10.1212/WNL.0000000000003509.
2. Maragkos, G.A., Geropoulos, G., Kechagias, K., Ziogas, I.A., Mylonas, K.S.: Quality of Life After Epilepsy Surgery in Children: A Systematic Review and Meta-Analysis. Neurosurg. 85, 741–749 (2019). https://doi.org/10.1093/neuros/nyy471.
3. Sheikh, S.R., McKee, Z.A., Ghosn, S., Jeong, K.-S., Kattan, M., Burgess, R.C., Jehi, L., Saab, C.Y.: Machine learning algorithm for predicting seizure control after temporal lobe resection using peri-ictal electroencephalography. Sci Rep. 14, 21771 (2024). https://doi.org/10.1038/s41598-024-72249-7.
4. Yossofzai, O., Fallah, A., Maniquis, C., Wang, S., Ragheb, J., Weil, A.G., Brunette-Clement, T., Andrade, A., Ibrahim, G.M., Mitsakakis, N., Widjaja, E.: Development and validation of machine learning models for prediction of seizure outcome after pediatric epilepsy surgery. Epilepsia. 63, 1956–1969 (2022). https://doi.org/10.1111/epi.17320.
5. Yan, H., Katz, J.S., Anderson, M., Mansouri, A., Remick, M., Ibrahim, G.M., Abel, T.J.: Method of invasive monitoring in epilepsy surgery and seizure freedom and morbidity: A systematic review. Epilepsia. 60, 1960–1972 (2019). https://doi.org/10.1111/epi.16315.
6. Guye, M., Régis, J., Tamura, M., Wendling, F., Gonigal, A.M., Chauvel, P., Bartolomei, F.: The role of corticothalamic coupling in human temporal lobe epilepsy. Brain. 129, 1917–1928 (2006). https://doi.org/10.1093/brain/awl151.
7. Pizzo, F., Roehri, N., Giusiano, B., Lagarde, S., Carron, R., Scavarda, D., McGonigal, A., Filipescu, C., Lambert, I., Bonini, F., Trebuchon, A., Bénar, C.-G., Bartolomei, F.: The Ictal Signature of Thalamus and Basal Ganglia in Focal Epilepsy: A SEEG Study. Neurology. 96, e280–e293 (2021). https://doi.org/10.1212/WNL.0000000000011003.
8. Edmonds, B., Miyakoshi, M., Gianmaria Remore, L., Ahn, S., Westley Phillips, H., Daida, A., Salamon, N., Bari, A., Sankar, R., Matsumoto, J.H., Fallah, A., Nariai, H.:

Characteristics of ictal thalamic EEG in pediatric-onset neocortical focal epilepsy. Clinical Neurophysiology. 154, 116–125 (2023). https://doi.org/10.1016/j.clinph.2023.07.007.
9. Ilyas, A., Pizarro, D., Romeo, A.K., Riley, K.O., Pati, S.: The centromedian nucleus: Anatomy, physiology, and clinical implications. J Clin Neurosci. 63, 1–7 (2019). https://doi.org/10.1016/j.jocn.2019.01.050.
10. Wu, T.Q., Kaboodvand, N., McGinn, R.J., Veit, M., Davey, Z., Datta, A., Graber, K.D., Meador, K.J., Fisher, R., Buch, V., Parvizi, J.: Multisite thalamic recordings to characterize seizure propagation in the human brain. Brain. 146, 2792–2802 (2023). https://doi.org/10.1093/brain/awad121.
11. Mohammadi, H., Karwowski, W.: Graph Neural Networks in Brain Connectivity Studies: Methods, Challenges, and Future Directions. Brain Sciences. 15, 17 (2025). https://doi.org/10.3390/brainsci15010017.
12. Bessadok, A., Mahjoub, M.A., Rekik, I.: Graph Neural Networks in Network Neuroscience. IEEE Transactions on Pattern Analysis and Machine Intelligence. 45, 5833–5848 (2023). https://doi.org/10.1109/TPAMI.2022.3209686.
13. Williamson, P.D.: Corpus Callosum Section For Intractable Epilepsy. In: Reeves, A.G. (ed.) Epilepsy and the Corpus Callosum. pp. 243–257. Springer US, Boston, MA (1985). https://doi.org/10.1007/978-1-4613-2419-5_10.
14. Fonov, V., Evans, A., McKinstry, R., Almli, C., Collins, D.: Unbiased nonlinear average age-appropriate brain templates from birth to adulthood. NeuroImage. 47, S102 (2009). https://doi.org/10.1016/S1053-8119(09)70884-5.
15. Fonov, V., Evans, A.C., Botteron, K., Almli, C.R., McKinstry, R.C., Collins, D.L.: Unbiased average age-appropriate atlases for pediatric studies. NeuroImage. 54, 313–327 (2011). https://doi.org/10.1016/j.neuroimage.2010.07.033.
16. Fedorov, A., Beichel, R., Kalpathy-Cramer, J., Finet, J., Fillion-Robin, J.-C., Pujol, S., Bauer, C., Jennings, D., Fennessy, F., Sonka, M., Buatti, J., Aylward, S., Miller, J.V., Pieper, S., Kikinis, R.: 3D Slicer as an image computing platform for the Quantitative Imaging Network. Magnetic Resonance Imaging. 30, 1323–1341 (2012). https://doi.org/10.1016/j.mri.2012.05.001.
17. McAuliffe, M.J., Lalonde, F.M., McGarry, D., Gandler, W., Csaky, K., Trus, B.L.: Medical Image Processing, Analysis and Visualization in clinical research. In: Proceedings 14th IEEE Symposium on Computer-Based Medical Systems. CBMS 2001. pp. 381–386 (2001). https://doi.org/10.1109/CBMS.2001.941749.
18. Gramfort, A., Luessi, M., Larson, E., Engemann, D.A., Strohmeier, D., Brodbeck, C., Goj, R., Jas, M., Brooks, T., Parkkonen, L., Hämäläinen, M.: MEG and EEG data analysis with MNE-Python. Front. Neurosci. 7, (2013). https://doi.org/10.3389/fnins.2013.00267.